Oral treatment with iododiflunisal delays beta amyloid plaque formation in a transgenic mouse model of Alzheimer Disease: a Longitudinal in vivo molecular imaging study

Luka Rejc
Univerza v Ljubljani
Vanessa Gómez-Vallejo
Centro de Investigacion Cooperativa en Biomateriales
Xabier Rios
Centro de Investigacion Cooperativa en Biomateriales
Unai Cossio
Centro de Investigacion Cooperativa en Biomateriales
Zuriñe Baz
Centro de Investigacion Cooperativa en Biomateriales
Edurne Mujica
Universidad del Pais Vasco
Tiago Giao
Universidade do Porto Instituto de Biologia Molecular e Celular
Ellen Y Cotrina
Instituto de Quimica Avanzada de Cataluna
Jesús Jiménez-Barbero
Center for Cooperative Research in Biosciences
Jordi Quintana
Universitat Pompeu Fabra
Gemma Arsequell
Instituto de Quimica Avanzada de Cataluna
Isabel Cardoso
Universidade do Porto Instituto de Biologia Molecular e Celular
Jordi Llop (jllop@cicbiomagune.es)
Centro de Investigacion Cooperativa en Biomateriales https://orcid.org/0000-0002-0821-9838

Research

Keywords: PET, positron emission tomography, Alzheimer disease, AD disease-modifying drug, transthyretin, small-molecule chaperones, TTR/Aβ interaction

Posted Date: February 10th, 2020

DOI: https://doi.org/10.21203/rs.2.23011/v1

TITLE

Oral treatment with iododiflunisal delays beta amyloid plaque formation in a transgenic mouse model of Alzheimer Disease: a Longitudinal in vivo molecular imaging study.

AUTHORS

Luka Rejc[1,*], Vanessa Gómez-Vallejo,[2] Xabier Rios,[2] Unai Cossio,[2] Zuriñe Baz,[2] Edurne Mujica,[3] Tiago Gião,[4,5] Ellen Y. Cotrina,[6] Jesús Jiménez-Barbero,[7,8,9] Jordi Quintana,[10,11] Gemma Arsequell,[6] Isabel Cardoso,[4,5,**] Jordi Llop[2,12,†]

AFFILIATIONS

[1] Faculty of Chemistry and Chemical Technology, University of Ljubljana, Slovenia.

[2] CIC biomaGUNE, Basque Research and Technology Alliance (BRTA), 20014 San Sebastian, Guipuzcoa, Spain.

[3] Biochemistry and Molecular Biology, EHU-UPV, Leioa, Spain.

[4] IBMC - Instituto de Biologia Molecular e Celular, Porto, Portugal.

[5] i3S – Instituto de Investigação e Inovação em Saúde, Universidade do Porto, Porto, Portugal.

[6] Institut de Química Avançada de Catalunya (I.Q.A.C.-C.S.I.C.), 08034 Barcelona, Spain

[7] CIC bioGUNE, Basque Research and Technology Alliance (BRTA), Bizkaia Technology Park, 48160 Derio, Bizkaia, Spain

[8] Ikerbasque, Basque Foundation for Science, Maria Diaz de Haro 3, 48013 Bilbao, Spain.

[9] Department Organic Chemistry II, Faculty Science & Technology, EHU-UPV, Leioa, Spain.

[10] Plataforma Drug Discovery, Parc Científic de Barcelona (PCB), Barcelona, Spain.

[11] Current affiliation: Research Programme on Biomedical Informatics, Universitat Pompeu Fabra, Barcelona, Spain

[12] Centro de Investigación Biomédica en Red – Enfermedades Respiratorias (CIBERES)

[*] e-mail: luka.rejc@fkkt.uni-lj.si; [**] icardoso@ibmc.up.pt; [†] jllop@cicbiomagune.es

ABSTRACT

Background: Transthyretin (TTR) is a tetrameric, Amyloid-beta (Aβ)-binding protein, which has been shown to reduce Aβ toxicity both *in vitro* and *in vivo*. The ability of TTR to interact with Aβ can be enhanced by a series of small molecules that stabilize its tetrameric form. Because of this, TTR stabilizers might act as disease modifying drugs in Alzheimer Disease (AD). In this work, we monitored the therapeutic efficacy of two TTR stabilizers, iododiflunisal (IDIF) and the repurposed drug tolcapone, by longitudinal assessment of Aβ deposition in an animal model of AD using positron emission tomography (PET) with [^{18}F]florbetaben.

Methods: Mice (AβPPswe/PS1A246E/TTR+/-; n=21) were divided into 3 groups (n=7 per group): iododiflunisal (IDIF)-treated, tolcapone-treated and non-treated. The treatment, administered in the drinking water at a dose of 100 mg/Kg/day, was started at 5 months of age. The level of Aβ deposition was assessed at ages=5, 9, 11, and 14 months by PET imaging using [^{18}F]florbetaben. Treatment efficacy was determined based on radiotracer uptake in the hippocampus (HIP) and the cortex (CTX) with respect to the cerebellum (CB) and presented as standardized uptake value ratios (SUVr). Immunohistochemical (IHC) analysis was performed at 14 months of age to further support *in vivo* results.

Results: SUVr of [^{18}F]florbetaben in CTX and HIP of non-treated animals progressively increased from age=5 to 11 months and stabilized afterwards. In contrast, [^{18}F]florbetaben uptake in HIP of IDIF-treated animals remained constant between ages=5 and 11 months and significantly increased at 14 months. At age=11 months, IDIF-treated group showed significantly lower SUVr values than those obtained for non-treated animals. In tolcapone-treated group, SUVr progressively increased with time, but at lower rate than in non-treated group. Moderate treatment effect of tolcapone suggests different mechanism of action than IDIF. No significant treatment effect was observed in CTX of IDIF- or tolcapone-treated animals. Results from IHC matched the *in vivo* data at age=14 months.

Conclusions: The TTR stabilizer IDIF shows good Aβ-protective effect. Nevertheless, Aβ levels in treated and control animals reached similar values at the end of the study. Furthermore, differences in efficacy between IDIF and tolcapone, suggest different mechanisms of action.

KEYWORDS.

PET, positron emission tomography, Alzheimer disease, AD disease-modifying drug, transthyretin, small-molecule chaperones, TTR/Aβ interaction.

MAIN TEXT

1. Background:

Alzheimer disease (AD) is the most common cause of dementia. It is the fifth leading cause of death globally, with a total of 2.4 million deaths in 2016, and the second leading

cause of death among those over the age of 70. Alarmingly, these numbers are increasing and are estimated to reach 50 million dementia patients by 2050, worldwide.

Pathophysiologically, AD is characterized by the accumulation of amyloid-beta (Aβ) aggregates (1), the occurrence of neurofibrillary tangles (NFTs) of hyperphosphorylated tau protein (2), and synaptic dysfunction (3). In addition, AD progression is accompanied by neuroinflammation (4), structural cerebrovascular alterations and deficits in cerebral glucose uptake and cerebral blood flow responses (5).

Knowledge gained on AD enabled the development of a variety of mechanism-based therapeutic approaches, which aim at slowing down or stopping the disease progression. Most investigated treatment strategies include: (i) minimizing the amount of Aβ in the brain by reducing its generation or accelerating its clearance from the brain; (ii) minimizing aggregation or post-translational modifications of tau protein; and (iii) inhibiting apolipoprotein E (ApoE) (6). Other neuroprotective strategies involve the use of neurotrophins and target neuroinflammation or oxidative stress. Nevertheless, despite decades of efforts, there is still no cure for AD. The outcome is especially worrying because over the last decade more than 50 drug candidates successfully passed phase II clinical trials but all failed in more advanced phases (7-11). Currently, there are only 132 agents in clinical trials for the treatment of AD (8) compared to more than 3558 drugs employed in cancer trials (12). The absence of approved disease-modifying therapy calls for an immediate intervention, by feeding new drug candidates into the currently exhausted AD drug development pipeline of stage I clinical trials.

Low success rate in finding appropriate treatment possibilities for AD could be overcome by the development of disease-modifying therapies (DMTs). One possibility of alleviating pathophysiological stress suggests reducing levels of Aβ and its toxic species

by enabling their transport out of the brain through the help of intrinsic proteins. Research in the past decade revealed that interactions of molecular chaperone proteins with toxic Aβ species minimize their harmful effects on the central nervous system (CNS) (13-16). Several intrinsic proteins were shown to be capable of modifying the stability/aggregation, circulation and clearance characteristics of Aβ peptides (17). Some examples of these proteins include Gelsolin (18), ApoJ (clusterin) (19, 20), ApoE (21), and human serum albumin (HSA) (22, 23). The latter was used by the healthcare company Grifols. They showed encouraging neuroimaging results in the AMBAR (Alzheimer Management by Albumin Replacement) clinical trial, indicating positive effects of HSA-Aβ interaction in patients with mild-to-moderate AD (24).

Another protein that helps transport Aβ peptides across the blood brain barrier (BBB) is Transthyretin (TTR) (25-28). TTR is a 55 kDa homotetramer (29) present in the serum and cerebrospinal fluid (CSF) and is the main Aβ binding protein in human CSF. It was demonstrated that the stability of the tetrameric form of TTR plays a pivotal role in amyloidogenic properties of the protein (30) and that unstable TTR complexes bind poorly to Aβ peptide (31). Studies on AD patients have shown that TTR has reduced ability to carry it's natural stabilizer, thyroxine (T_4) in blood plasma (32) and that the ratio folded/monomeric TTR is reduced in AD patients (33). This indicates that TTR stability affect neuroprotective ability of the tetramer. Indeed, the presence of resveratrol led to deceleration of TTR clearance and restoration of normal concentration levels of TTR in the brain (34), possibly due to favored dimer-dimer interaction, which supports tetrameric form of TTR. The seemingly positive effect of increased stability of TTR tetrameric form on TTR-Aβ interaction opens a new avenue for targeting disease pathogenesis.

With the aim of providing a prioritized list of compounds that help enhance the TTR/Aβ interaction, we started a drug discovery program using a combination of computational modeling, *in vitro* affinity/selectivity/stability assays and structural studies (35). One of these compounds, iododiflunisal (IDIF; Figure 1) has proven efficient in promoting Aβ clearance from the brain and improving animal's cognitive functions when orally administered to AD transgenic mice (AβPPswe/PS1A246E/TTR+/-) daily for 2 months, starting just before the onset of the disease (36). Another study showed that the formation of TTR-IDIF complex enhances brain penetration of both TTR and IDIF (37). These results suggest that IDIF stabilizes TTR *in vivo* and prevents Aβ deposition in the brain. On the other hand, tolcapone (Figure 1), a selective, potent and reversible nitrocatechol-type inhibitor of the enzyme catechol-*O*-methyltransferase, originally used for the treatment of Parkinson disease, was shown to stabilize TTR *in vitro* (38) and is currently being repurposed for the treatment of TTR-related amyloidosis (39).

The studies so far lacked longitudinal *in vivo* assessment of efficacy and long-term effects of treatment. Here, we present longitudinal *in vivo* evaluation of the therapeutic efficacy of IDIF and tolcapone upon oral administration to AD transgenic mice after the onset of the disease. The same transgenic AD mouse model (AβPPswe/PS1A246E/TTR+/-) and the same dosing regimen were used as in our previous study (36). The concentration of Aβ plaques in the brain was longitudinally monitored by means of the non-invasive, ultra-sensitive *in vivo* imaging technique Positron Emission Tomography (PET). The validated radiotracer [^{18}F]florbetaben, previously used for imaging Aβ plaques in AD patients (40), different transgenic AD mouse models (41-46) and also in longitudinal therapeutic efficacy studies of AD transgenic mouse models (47), was used for assessing protein aggregates distribution.

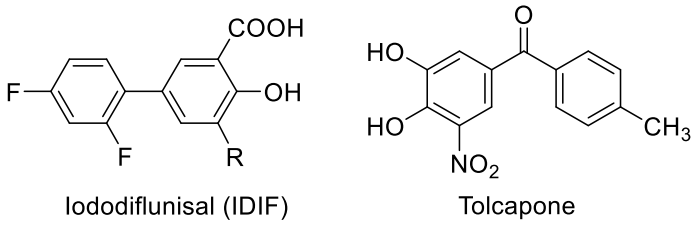

Figure 1. TTR tetramer stabilizers: small T_4-like molecules iododiflunisal (IDIF) and repurposed drug tolcapone.

2. Methods

2.1 Compounds

IDIF meglumine salt was prepared as previously described (36). In brief, to a solution of *N*-methyl-D-glucamine (meglumine) (1.22 g, 6.23 mmol) in water (2 mL), ethanol (0.5 mL) and IDIF (2.34 g, 4.23 mmol) were added over 15 min in small portions. The solution was stirred for 2 h, evaporated under reduced pressure and frozen. Tolcapone was isolated from the registered drug Tasmar (MEDA Pharma). In brief, the pills were triturated in the presence of ethyl acetate. The solution was filtered and the filtrate evaporated under reduced pressure. The corresponding meglumine salt was prepared in the same way as reported for IDIF meglumine salt. Purity of all final compounds was proved to be ≥95% by means of high performance liquid chromatography (HPLC), high-resolution mass spectrometry (HR-MS) and nuclear magnetic resonance (NMR) spectroscopy.

2.2 Radiolabeling

[^{18}F]Florbetaben was prepared by ^{18}F-fluorination/hydrolysis of the *N*-BOC-protected precursor, prepared as previously described (48) with minor modifications. The

radiosynthesis was performed using a TRACERlab FX_{FN} synthesis module (GE Healthcare). $[^{18}F]F^-$ was first trapped on a pre-conditioned Sep-Pak® Accell Plus QMA Light cartridge (Waters, Milford, MA, USA), and then eluted with a solution of Kryptofix $K_{2.2.2}/K_2CO_3$ in a mixture of water and acetonitrile. After complete elimination of the solvent by azeotropic evaporation, a solution containing the precursor (3 mg) in dimethylsulfoxide (1 mL) was added and the mixture was heated at 165°C for 5 min. The reactor was then cooled at room temperature, 10% HCl aqueous solution was added (0.25 mL) and the mixture was heated (2.5 min, 90°C). The reaction crude was then diluted with NaOH solution (0.33 mL, 0.1 g/mL) and 3 mL of mobile phase, and purified by HPLC using a Nucleosil 100-7 C18 column (Macherey-Nagel, Düren, Germany) as stationary phase and aqueous ascorbate buffer solution (20 g of ascorbic acid + 4,54 g NaOH in 2 L water, pH adjusted to 8.7 with 0.1 M NaOH; this solution diluted 1:1 with water)/acetonitrile (40/60, V/V) as the mobile phase at a flow rate of 5 mL/min. The desired fraction (retention time = 29–30 min) was collected, diluted with water (20 mL), and the radiotracer was retained on a C-18 cartridge (Sep-Pak® Light, Waters, Milford, MA, USA) and further eluted with ethanol (1 mL) and ascorbate buffer solution (20 g of ascorbic acid + 4,54 g NaOH in 2 L water, pH adjusted to 8.7 with 0.1 M NaOH; 5 mL). Filtration through a 0.22 μm filter yielded the final solution, ready for injection. Chemical and radiochemical purity were determined by HPLC using an Agilent 1200 Series system equipped with a radioactivity detector (Gabi, Raytest) and a variable wavelength detector (λ = 350 nm) connected in series. A RP-C18 column (Mediterranea Sea 18, 4.6×150 mm, 5 μm particle size; Teknokroma, Spain) was used as the stationary phase and ascorbate buffer solution (20 g of ascorbic acid + 4.54 g NaOH in 2 L water, pH adjusted to 8.7 with 0.1 M NaOH; this solution diluted 1:1 with water)/acetonitrile (40/60, V/V) as the mobile phase (retention time = 6.0 min).

2.3 Animals and study design

Animals were maintained and handled in accordance with the Guidelines for Accommodation and Care of Animals (European Convention for the Protection of Vertebrate Animals Used for Experimental and Other Scientific Purposes). All animal procedures were performed in accordance with the European Union Animal Directive (2010/63/EU). Experimental procedures were approved by the corresponding Ethical Committees.

The mouse model AβPPswe/PS1A246E/TTR+/- (carrying only one copy of the TTR gene), was generated as previously described (36) by crossing AβPPswe/PS1A246E transgenic mice (49) (B6/C3H background) purchased from The Jackson Laboratory with TTR-null mice (TTR−/−) (SV129 background) (50). Mice were bred at I3S (Porto, Portugal) and transferred to CIC biomaGUNE (San Sebastian, Spain) at 4–5 months of age to apply treatments and conduct imaging studies. Upon arrival, mice were randomly divided into three groups: Group I, non-treated (n=7); group II, IDIF-treated (n=7); and group III, tolcapone-treated (n=7) mice. The treatment was introduced in the drinking water at a concentration of 575 mg of meglumine IDIF salt and 575 mg meglumine tolcapone salt per liter (2.8 mg drug/rodent/day).

The disease progression was followed using PET-[^{18}F]florbetaben at the age of 5, 9, 11 and 14 months. All the animals were sacrificed when they reached human endpoint of the disease, but no later than 15 months of age; the same criterion was used for all three groups of animals.

2.4 PET-CT imaging

Imaging experiments were performed using an eXplore Vista-CT small animal PET-CT system (GE Healthcare). In all cases, anaesthesia was induced with 3% isoflurane in

pure oxygen and maintained during imaging studies with 1.5–2.0% isoflurane in pure oxygen. Mice were injected intravenously (IV) with [^{18}F]florbetaben (10–20 MBq; injected volume: 100–150 µL). At each time point, a 30-min static PET image was acquired 30 min post IV injection in one bed position to assess the accumulation in the brain (energy range 400–700 keV). A CT scan was acquired immediately after PET acquisition (X-Ray energy: 40 kV, intensity: 140 µA). PET images were reconstructed using filtered back projection (FBP) applying random, scatter, and attenuation corrections.

PET images were co-registered with a magnetic resonance imaging (MRI) template (M. Mirrione-T2, available in the π-MOD image processing tool) and different brain regions (cortex, hippocampus, cerebellum, whole brain) were automatically delineated. The concentration of activity was determined in each region and expressed as Standard Uptake Value (SUV). Treatment efficacy was determined based on the amount of [^{18}F]florbetaben in different brain regions. The hippocampus (HIP) and cortex (CTX) were chosen as brain regions of interest. The cerebellum (CB) was chosen as reference region. Aβ plaque abundance was determined as relative SUV (SUVr) of [^{18}F]florbetaben in HIP and CTX with respect to CB.

2.5 Immunohistochemical analysis

Aβ plaque burden was evaluated by performing free-floating immunohistochemistry assay on 30 µm-thick cryostat coronal brain sections, using monoclonal biotinylated Aβ1-16 antibody (6E10) (Covance Research Products, Inc.), as previously described (51). In brief, free-floating brain sections were washed twice in phosphate-buffered saline (PBS), and once in distilled water (dH_2O). For partial amyloid denaturation, 70% formic acid (FA) was used for 15 min at room temperature, with gentle agitation. After

washing in dH_2O and then PBS, endogenous peroxidase activity was inhibited with 1% hydrogen peroxide (H_2O_2) in PBS for 20 min. Following PBS washes, sections were blocked in blocking solution (10% fetal bovine serum (FBS) and 0.5% Triton X-100) for 1 h at room temperature and then incubated with biotinylated 6E10 primary antibody overnight at 4 °C, with gentle agitation. Sections were washed with PBS and incubated in Vectastain® Elite ABC Reagent (Vector Laboratories, Inc.). After washing once more with PBS, sections were developed with diaminobenzidine (Sigma-Aldrich, Inc.), mounted on 0.1% gelatin-coated slides and dried overnight at room temperature. After dehydration, slides were coverslipped under Entellan® (Merck & Co., Inc.) and examined using an Olympus BX50 light microscope. Plaque burden was evaluated using Image-Pro Plus software, by analyzing the immunostained area fraction in the HIP and CTX (expressed as percentage of analyzed area) of five sections per animal.

2.6 Statistical analysis

Statistical significance of differences in between time points (for each treatment) or treatment (at a single time point) was calculated using t-student test analyses. $P < 0.05$ was considered significant.

3. Results

3.1 PET-CT imaging

Longitudinal PET-CT imaging using [^{18}F]florbetaben was carried out to determine the Aβ plaque burden at the whole brain level and in selected brain subregions *in vivo*. Animals submitted to different treatments were scanned at 5, 9, 11 and 14 months of age.

A steady decrease of [^{18}F]florbetaben uptake over time was observed in the whole brain in all animal groups (Figures 2a and 2d–2g). SUV values decreased from ca. 0.1 at age=5

months to ca. 0.05 at age=14 months. No significant differences among groups were observed at any age. Similar trends were observed for SUV values obtained for CTX (Figure 2b) and HIP (Figure 2c).

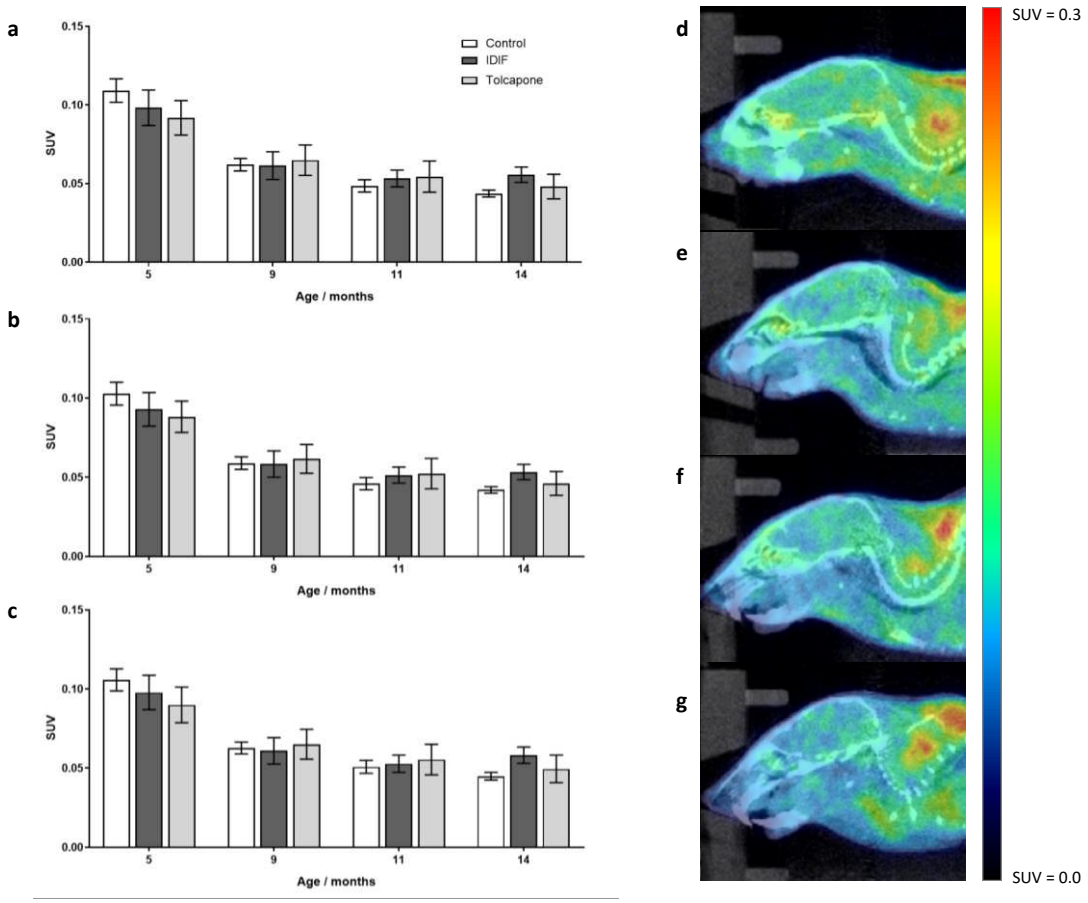

Figure 2. (a–c) SUV values obtained after administration of [^{18}F]florbetaben in: (a) the whole brain; (b) the cortex; and (c) the hippocampus of non-treated, IDIF-treated and tolcapone-treated mice at different ages; (d–g) Representative sagittal PET-CT images obtained at ages of 5 (d), 9 (e), 11 (f) and 14 (g) months after administration of [^{18}F]florbetaben. Images shown correspond to one non-treated animal.

SUVr values (determined as the ratio between SUV values in the investigated region and CB) in CTX progressively increased with age, irrespective of the treatment received by

the animals (Figure 3a). Differences between groups at a given age or between ages within each group were not significant.

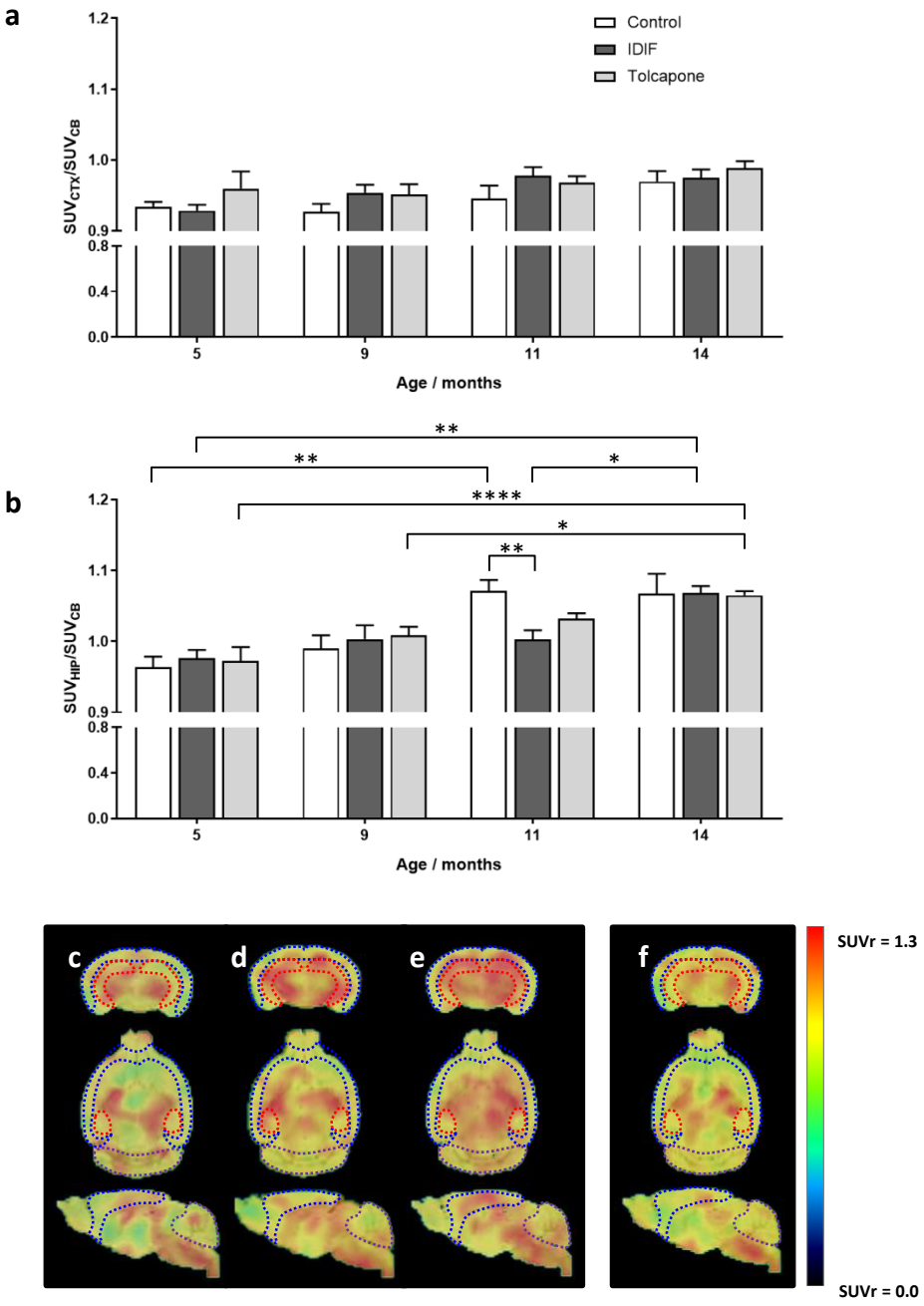

Figure 3. SUVr values (SUV values relative to the cerebellum) in the cortex (a) and the hippocampus (b), obtained after administration of [^{18}F]florbetaben to non-treated, IDIF-treated and tolcapone-treated mice at different ages; (c-f) representative axial, coronal and sagittal PET images corresponding to a non-treated animals at ages=9 (c), 11 (d) and 14 (e) months; (f) representative PET image for an IDIF-treated mouse at the age of 11 months. PET images have

been co-registered with a brain mouse atlas. Volumes of interest drawn in the cortex (blue), hippocampus (red) and cerebellum (brown) are displayed.

SUVr values in CTX were always below 1, indicating that the radiotracer uptake in CTX is actually lower than the uptake in CB. In contrast, SUVr values determined for HIP showed significant differences between groups (Figure 3b). For non-treated animals, values progressively increase from age=5 months (0.96±0.04) to age=11 months (1.07±0.03) (P=0.005) and stabilize afterwards (1.067±0.05 at age=14 months). For IDIF-treated animals, the trend is different. Values rise from 0.98±0.03 at age=5 months to 1.00±0.03 at age=11 months (non-significant increase, P=0.61), and dramatically increase afterwards to reach a value of 1.07±0.02 at the age of 14 months (P=0.03 vs. SUVr at age=11 months; P=0.0027 vs. SUVr at age=5 months). Finally, tolcapone-treated animals show a trend that lies in between those observed for non-treated and IDIF-treated animals. For this group values progressively increase with time, resulting in SUVr values 0.97±0.05, 1.01±0.03, 1.03±0.02 and 1.065±0.015 at 5, 9, 11 and 14 months, respectively. Noteworthy, SUVr values obtained at 11 and 14 months significantly differ from those obtained at 5 months (P=0.012 and <0.001, respectively). At the age of 11 months, SUVr values obtained for IDIF-treated animals (1.00±0.03) are significantly lower than those obtained for non-treated animals (1.07±0.03; P=0.0045) (see Figures 3c-3f for representative images).

3.2 Immunohistochemistry

The effect of the treatment on Aβ deposition was studied by assessing Aβ burden in all animals after the last imaging session (age=14 months) by immunohistochemical (IHC) analyses followed by quantification. IHC did not show any significant differences between treated and non-treated animals at this time point, neither in CTX (Figure 4a)

nor in HIP (Figure 4b). In all cases, high plaque density was observed, with significant variability among individuals, as observed in the photomicrographs (Figure 4c).

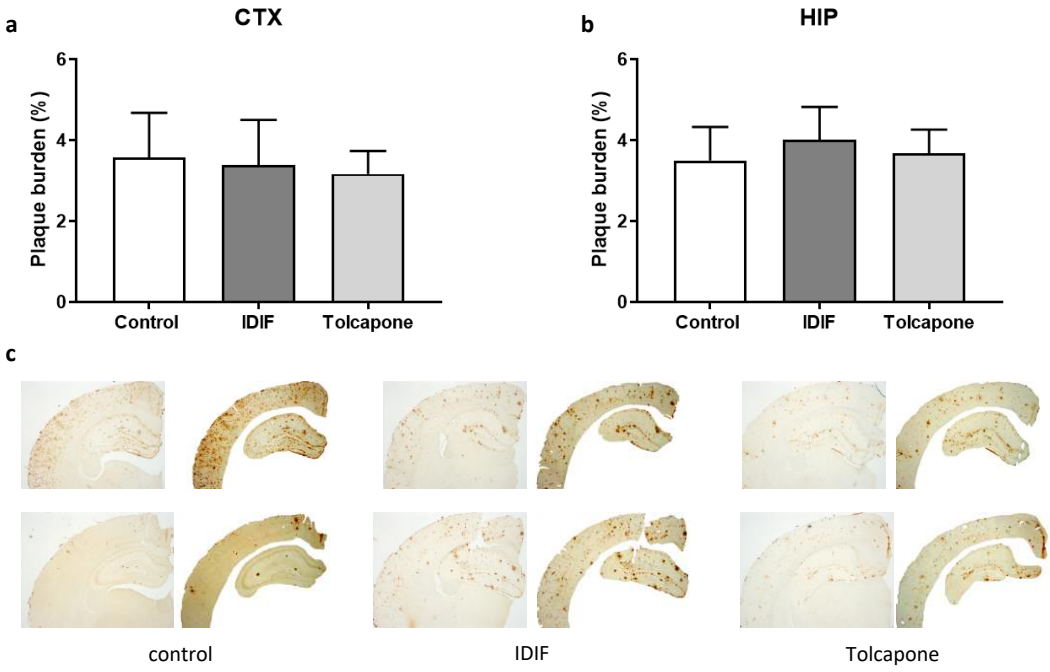

Fig. 4. (a, b) Aβ plaque burden in the cortex and hippocampus of non-treated (control), IDIF-treated and tolcapone-treated mice at age=14 months. Error bars represent SEM; (c) photomicrographs illustrate immunohistochemical analysis of brain Aβ plaques using the 6E10 antibody. Brain slices (left) and selected areas for quantification (right) are shown. Slides within each group correspond to two representative animals.

4. Discussion

TTR is an important transporter protein for the brain defense against pathophysiological stress caused by Aβ deposition. Previous studies on AD animal models have shown that oral administration of IDIF, a TTR tetramer-stabilizing drug, results in decreased Aβ plaque deposition and ameliorates cognitive status at early stages of the disease (36). To fully evaluate the potential of IDIF to act as a disease-modifying drug, longitudinal therapeutic efficacy and long-term treatment effect on

plaque deposition was assessed by PET-[^{18}F]florbetaben imaging. Additionally, a possible use of tolcapone as a repurposed drug for TTR stabilization was investigated.

Similar to previous preclinical PET-[^{18}F]florbetaben studies (41-43, 45), SUVr values (calculated as the ratio between SUV in the region of interest and SUV in the reference region, CB) were calculated and used as a surrogate of plaque density in different brain regions. Plaque density was determined in CTX and HIP, areas that are the most affected by the protein deposition in AD.

PET-[^{18}F]florbetaben imaging showed progressive decrease of uptake in the whole brain with age, both in control (non-treated) and treated animals (Figure 2a). Similar trend was observed in CTX and HIP (Figures 2b–2c). Considering the expected increase in plaque load with age, at least in non-treated animals, this was against our expectations. To the best of our knowledge longitudinal studies of absolute SUV values have not yet been reported for this radiotracer; however, a study reporting the use of structurally similar radiotracer, [^{18}F]AV45, for monitoring amyloid pathology (52, 53), showed the opposite trend. In their work (52), authors observed an increase in tracer uptake in CTX, HIP and thalamus (THA) of APPPS1-21 double transgenic mice (which co-express the human Swedish double APP mutation KM670/671NL and the human mutated PS1 L166P driven by the neuron-specific Thy-1 promoter) from 8 to 13 months of age. The reasons behind the discrepancy between the two studies are unknown, but the most plausible cause for this phenomenon may stem from the inherent differences between the two animal models. Our hypothesis is that there are physiological factors that contribute to decreased tracer uptake in parallel to disease progression. Such physiological changes have indeed been reported in AD mice models (54).

In evaluation of treatment efficacy, the effects of intrinsic genetic differences between animal models were avoided by presenting the data as SUV of [^{18}F]florbetaben in CTX and HIP with respect to CB (SUVr) (41-43, 45). SUVr values in CTX and HIP of non-treated animals progressively increased with animal age (Figures 3a–3b). Similar to previously reported studies in a different animal model (42), significant differences were only observed in HIP but not in CTX. PET images obtained at 9, 11 and 14 months (Figures 3c–3f) clearly showed an increase in SUVr values in HIP of non-treated animals from 9 to 11 months, while the increase in plaque load from 11 to 14 months was not apparent, according to quantification data.

As for the treatment groups, IDIF-treatment delayed Aβ plaque build-up in HIP until the age=11 months, but could not fight severe plaque accumulation at later stages. IHC analysis at the end point confirmed that there were no significant differences between IDIF-treated and non-treated animal groups (Figure 4). The absence of differences between non-treated and IDIF-treated animals at the end point is most likely not related to inability of stabilizers to complete their task. There are many possible reasons behind these results, including the occurrence of other disease-related processes that possibly take over the main role at more advanced stages of the disease. Although not proven, factors such as a decrease in fluid intake as a consequence of the phenotype (which has been reported for other AD models (55)) or hindered mobility, may lead to lower drug intake and hence limited therapeutic efficacy.

Importantly, no clear evidence of Aβ protein clearance was observed in tolcapone-treated group. Compared to non-treated animals, tolcapone helped slow down the rate of plaque deposition in HIP, suggesting some protective effects of the treatment. Even though previous report showed that tolcapone and entacapone inhibit Aβ fibrilization in

a specific and concentration-dependent manner (56), our results suggest that direct effect of tolcapone was not sufficient to produce significant differences between treated and non-treated animals. Difference in effectiveness, when compared to IDIF, suggests a different mechanism of action. Although *in vitro* studies have shown that tolcapone stabilizes TTR tetramer, limited chaperoning ability in TTR/Aβ interaction could be the cause of the inability of tolcapone-TTR complex to promote Aβ clearance from the brain. This hypothesis is supported by our recent work describing the lack of chaperoning capabilities of TTR/Aβ interaction of the orphan drugs Tafamidis and diflunisal *in vitro*, although they are both TTR stabilizers (57).

The positive IDIF treatment effect observed in HIP was not matched in CTX. It seems that CTX was not affected by either of the treatments. This is not surprising, since some studies show differences in the amount of TTR in different brain regions (58). Furthermore, our recent PET-imaging study shows that entrance of TTR into the brain after intravenous administration starts at the third ventricles, which suggests that TTR traffic occurs partially via the cerebrospinal fluid-brain barrier (CSFBB) and not only through the blood brain barrier (BBB) (37). Ultimately, this led to lower and delayed TTR presence in peripheral areas of the brain (37), such as CTX, where a significant concentration of TTR could be observed only at 6 hours after administration. Assuming the same transport mechanism of IDIF- and tolcapone-stabilized TTR this delay could be one of the reasons for insufficient influx of the complex into CTX. In turn, this would lead to ineffective Aβ clearance, resulting in the absence of differences between treated and non-treated mice.

Of note, *in vivo* results show lower increase in SUVr in CTX compared to HIP over time. *Ex vivo* IHC staining at 14 months of age did not corroborate these findings. Contrarily,

no significant difference in abundance of Aβ was found between CTX and HIP. The differences between *in vivo* and *ex vivo* results could be due to different tissue permeability in different brain regions. This would impede uniform radiotracer distribution throughout the brain *in vivo* and could cause differences in [^{18}F]florbetaben wash-out rates. Investigation of possible reasons for the observed findings is out of the scope of this work and will be addressed in future studies.

5. Conclusions

In conclusion, this is the first large-scale longitudinal Aβ-PET study of cerebral amyloidosis in a transgenic AD mouse model, treated with small molecules that enhance TTR/Aβ interaction. Our work confirms positive effects of TTR stabilizers IDIF and (to a minor extent) tolcapone on delay and/or slowing down Aβ deposition. Furthermore, this study offers the first evidence of how the ability to stabilize TTR complexes affects the degree of amyloidosis in the brain longitudinally. The results suggest that IDIF behaves as chaperone of the TTR-Aβ interaction and could be used to ameliorate Aβ aggregate-related pathological stress by promoting amyloid plaque clearance from CNS.

Furthermore, the present study provides with the basis for the design of a dose-response study and translation of this new disease-modifying approach to clinical trials for AD therapy. It also shows a great significance of development of small, T_4-like structures for new therapeutic strategies against AD.

6. List of abbreviations

Aβ: Amyloid beta

AD: Alzheimer's disease

BBB: Blood-brain barrier

CB: Cerebellum

CSF: Cerebrospinal fluid

CSFBB: Cerebrospinal fluid-blood barrier

CT: Computed tomography

DMT: Disease-modifying therapy

FBP: Filtered back projection

HSA: Human serum albumin

HIP: Hippocampus

HPLC: high pressure liquid chromatography

IDIF: Iododiflunisal

IHC: immunohistochemistry

MRI: Magnetic resonance imaging

NFT: Neurofibrillary tangles

PET: Positron emission tomography

SUV: Standardized uptake value

SUVr: Relative standardized uptake value (to a region of reference)

TTR: Transthyretin

7. Declarations

7.1 Ethics approval and consent to participate,

All animal experiments were approved by the Ethical Committee of CIC biomaGUNE and by the local authorities (Diputación Foral de Guipúzcoa; authorization number: PRO-AE-SS-084).

7.2 Consent for publication

Not applicable

7.3 Availability of data and materials

The datasets used and/or analyzed during the current study are available from the corresponding author on reasonable request

7.4 Competing interests

The authors declare that they have no competing interests

7.5 Funding

The work was supported by a grant from the Fundació Marató de TV3 (Neurodegenerative Diseases Call, Project Reference 20140330-31-32-33-34, http://www.ccma.cat/tv3/marato/en/ projectes-financats/2013/212/). The group at CIC biomaGUNE also acknowledges The Spanish Ministry of Economy and Competitiveness for funding through Grant CTQ2017-87637-R. I. Cardoso worked under the Investigator FCT Program which is financed by national funds through the Foundation for Science and Technology (FCT, Portugal) and co-financed by the European Social Fund (ESF) through the Human Potential Operational Programme (HPOP), type 4.2 - Promotion of Scientific Employment. G. Arsequell acknowledges financial support from the Spanish Ministry of Economy (CTQ2016-76840-R). E.Y. Cotrina acknowledges a contract from Fundació Marató de TV3, Spain (Project ref.

20140330-31-32-33-34) and a one year contract from Ford-Fundación Apadrina la Ciencia.

7.6 Authors' contributions

J. L, L. R., I. C. and G. A. designed the study, interpreted the data and wrote the manuscript. X. R. and V. G.-V. performed radiochemical syntheses. U.C. performed PET-CT experiments. Z. B. and E. M. carried out image analysis and quantification. I. C. and T. G. performed IHC analysis and contributed to interpretation of the results. J. Q., J. J.-B. and E. Y. Cotrina participated in study design, data interpretation and revision of the manuscript. All authors have given approval to the final version of the manuscript.

7.7 Acknowledgements

The authors thank the animal facility staff at CIC biomaGUNE for administration of the compounds; Aitor Lekuona and Víctor Salinas for assistance in cyclotron operation and automated syntheses; and Prof. Dr. A. Ballesteros (University of Oviedo, Oviedo, Spain) for support on the IDIF synthesis.

8. References

1. Selkoe DJ, Hardy J. The amyloid hypothesis of Alzheimer's disease at 25 years. EMBO Mol Med. 2016;8(6):595-608. Epub 2016/03/31.

2. Goedert M, Spillantini MG, Cairns NJ, Crowther RA. Tau proteins of Alzheimer paired helical filaments: abnormal phosphorylation of all six brain isoforms. Neuron. 1992;8(1):159-68. Epub 1992/01/01.

3. Forner S, Baglietto-Vargas D, Martini AC, Trujillo-Estrada L, LaFerla FM. Synaptic Impairment in Alzheimer's Disease: A Dysregulated Symphony. Trends Neurosci. 2017;40(6):347-57. Epub 2017/05/13.

4. McGeer EG, McGeer PL. Inflammatory processes in Alzheimer's disease. Prog Neuropsychopharmacol B□ol Psychiatry. 2003;27(5):741-9. Epub 2003/08/19.

5. Koizumi K, Wang G, Park L. Endothelial Dysfunction and Amyloid-beta-Induced Neurovascular Alterations. Cell Mol Neurobiol. 2016;36(2):155-65. Epub 2015/09/04.

6. Cao J, Hou J, Ping J, Cai D. Advances in developing novel therapeutic strategies for Alzheimer's disease. Molecular Neurodegeneration. 2018;13(1):64.

7. Cummings J. Lessons Learned from Alzheimer Disease: Clinical Trials with Negative Outcomes. Clin Transl Sci. 2018;11(2):147-52. Epub 2017/08/03.

8. Cummings J, Lee G, Ritter A, Sabbagh M, Zhong K. Alzheimer's disease drug development pipeline: 2019. Alzheimer's and Dementia: Translational Research and Clinical Interventions. 2019;5:272-93.

9. Cummings J, Ritter A, Zhong K. Clinical Trials for Disease-Modifying Therapies in Alzheimer's Disease: A Primer, Lessons Learned, and a Blueprint for the Future. J Alzheimers Dis. 2018;64(s1):S3-S22. Epub 2018/03/23.

10. Molinuevo JL, Minguillon C, Rami L, Gispert JD. The Rationale behind the New Alzheimer's Disease Conceptualization: Lessons Learned during the Last Decades. J Alzheimer's Dis. 2018;62(3):1067-77.

11. Mehta D, Jackson R, Paul G, Shi J, Sabbagh M. Why do trials for Alzheimer's disease drugs keep failing? A discontinued drug perspective for 2010-2015. Expert Opinion on Investigational Drugs. 2017;26(6):735-9.

12. Cummings J, Feldman HH, Scheltens P. The "rights" of precision drug development for Alzheimer's disease. Alzheimer's Research and Therapy. 2019;11(1).

13. Mannini B, Cascella R, Zampagni M, Van Waarde-Verhagen M, Meehan S, Roodveldt C, et al. Molecular mechanisms used by chaperones to reduce the toxicity of aberrant protein oligomers. Proc Natl Acad Sci U S A. 2012;109(31):12479-84.

14. Narayan P, Meehan S, Carver JA, Wilson MR, Dobson CM, Klenerman D. Amyloid-β oligomers are sequestered by both intracellular and extracellular chaperones. Biochemistry (Mosc). 2012;51(46):9270-6.

15. Cohen SIA, Arosio P, Presto J, Kurudenkandy FR, Biverstål H, Dolfe L, et al. A molecular chaperone breaks the catalytic cycle that generates toxic Aβ oligomers. Nature Structural and Molecular Biology. 2015;22(3):207-13.

16. Arosio P, Michaels TCT, Linse S, Månsson C, Emanuelsson C, Presto J, et al. Kinetic analysis reveals the diversity of microscopic mechanisms through which molecular chaperones suppress amyloid formation. Nature Communications. 2016;7.

17. Watts G. Prospects for dementia research. Lancet (London, England). 2018;391(10119):416.

18. Ji L, Zhao X, Hua Z. Potential therapeutic implications of gelsolin in Alzheimer's disease. J Alzheimer's Dis. 2015;44(1):13-25.

19. Nelson AR, Sagare AP, Zlokovic BV. Role of clusterin in the brain vascular clearance of amyloid-beta. Proc Natl Acad Sci U S A. 2017;114(33):8681-2. Epub 2017/08/03.

20. Beeg M, Stravalaci M, Romeo M, Carra AD, Cagnotto A, Rossi A, et al. Clusterin Binds to Abeta1-42 Oligomers with High Affinity and Interferes with Peptide Aggregation by Inhibiting Primary and Secondary Nucleation. J Biol Chem. 2016;291(13):6958-66. Epub 2016/02/18.

21. Liu S, Park S, Allington G, Prelli F, Sun Y, Marta-Ariza M, et al. Targeting Apolipoprotein E/Amyloid beta Binding by Peptoid CPO_Abeta17-21 P Ameliorates Alzheimer's Disease Related Pathology and Cognitive Decline. Sci Rep. 2017;7(1):8009. Epub 2017/08/16.

22. Boada M, Anaya F, Ortiz P, Olazaran J, Shua-Haim JR, Obisesan TO, et al. Efficacy and Safety of Plasma Exchange with 5% Albumin to Modify Cerebrospinal Fluid and Plasma

Amyloid-beta Concentrations and Cognition Outcomes in Alzheimer's Disease Patients: A Multicenter, Randomized, Controlled Clinical Trial. J Alzheimers Dis. 2017;56(1):129-43. Epub 2016/12/03.

23. Algamal M, Ahmed R, Jafari N, Ahsan B, Ortega J, Melacini G. Atomic-resolution map of the interactions between an amyloid inhibitor protein and amyloid beta (Abeta) peptides in the monomer and protofibril states. J Biol Chem. 2017;292(42):17158-68. Epub 2017/08/12.

24. Boada M, López O, Núñez L, Szczepiorkowski ZM, Torres M, Grifols C, et al. Plasma exchange for Alzheimer's disease Management by Albumin Replacement (AMBAR) trial: Study design and progress. Alzheimer's and Dementia: Translational Research and Clinical Interventions. 2019;5:61-9.

25. Schwarzman AL, Gregori L, Vitek MP, Lyubski S, Strittmatter WJ, Enghilde JJ, et al. Transthyretin sequesters amyloid beta protein and prevents amyloid formation. Proc Natl Acad Sci U S A. 1994;91(18):8368-72. Epub 1994/08/30.

26. Stein TD, Johnson JA. Lack of neurodegeneration in transgenic mice overexpressing mutant amyloid precursor protein is associated with increased levels of transthyretin and the activation of cell survival pathways. J Neurosci. 2002;22(17):7380-8.

27. Buxbaum JN, Ye Z, Reixach N, Friske L, Levy C, Das P, et al. Transthyretin protects Alzheimer's mice from the behavioral and biochemical effects of Aβ toxicity. Proc Natl Acad Sci U S A. 2008;105(7):2681-6.

28. Alemi M, Gaiteiro C, Ribeiro CA, Santos LM, Gomes JR, Oliveira SM, et al. Transthyretin participates in beta-amyloid transport from the brain to the liver-involvement of the low-density lipoprotein receptor-related protein 1? Scientific Reports. 2016;6.

29. Saraiva MJM. Transthyretin amyloidosis: A tale of weak interactions. FEBS Lett. 2001;498(2-3):201-3.

30. Almeida MR, Gales L, Damas AM, Cardoso I, Saraiva MJ. Small transthyretin (TTR) ligands as possible therapeutic agents in TTR amyloidoses. Curr Drug Targets: CNS Neurol Disorders. 2005;4(5):587-96.

31. Schwarzman AL, Tsiper M, Wente H, Wang A, Vitek MP, Vasiliev V, et al. Amyloidogenic and anti-amyloidogenic properties of recombinant transthyretin variants. Amyloid. 2004;11(1):1-9.

32. Ribeiro CA, Santana I, Oliveira C, Baldeiras I, Moreira J, Saraiva MJ, et al. Transthyretin decrease in plasma of MCI and AD patients: Investigation of mechanisms for disease modulation. Current Alzheimer Research. 2012;9(8):881-9.

33. Alemi M, Silva SC, Santana I, Cardoso I. Transthyretin stability is critical in assisting beta amyloid clearance– Relevance of transthyretin stabilization in Alzheimer's disease. CNS Neuroscience and Therapeutics. 2017;23(7):605-19.

34. Santos LM, Rodrigues D, Alemi M, Silva SC, Ribeiro CA, Cardoso I. Resveratrol administration increases transthyretin protein levels, ameliorating AD features: The importance of transthyretin tetrameric stability. Mol Med. 2016;22:597-607.

35. Gimeno A, Santos LM, Alemi M, Rivas J, Blasi D, Cotrina EY, et al. Insights on the Interaction between Transthyretin and Aβ in Solution. A Saturation Transfer Difference (STD) NMR Analysis of the Role of Iododiflunisal. J Med Chem. 2017;60(13):5749-58.

36. Ribeiro CA, Oliveira SM, Guido LF, Magalhaes A, Valencia G, Arsequell G, et al. Transthyretin stabilization by iododiflunisal promotes amyloid-beta peptide clearance, decreases its deposition, and ameliorates cognitive deficits in an Alzheimer's disease mouse model. J Alzheimers Dis. 2014;39(2):357-70. Epub 2013/10/31.

37. Rios X, Gómez-Vallejo V, Martín A, Cossío U, Morcillo MÁ, Alemi M, et al. Radiochemical examination of transthyretin (TTR) brain penetration assisted by iododiflunisal, a TTR tetramer stabilizer and a new candidate drug for AD. Scientific Reports. 2019;9(1).

38. Sant'Anna R, Gallego P, Robinson LZ, Pereira-Henriques A, Ferreira N, Pinheiro F, et al. Repositioning tolcapone as a potent inhibitor of transthyretin amyloidogenesis and associated cellular toxicity. Nature Communications. 2016;7.

39. Gamez J, Salvadó M, Reig N, Suñé P, Casasnovas C, Rojas-Garcia R, et al. Transthyretin stabilization activity of the catechol-O-methyltransferase inhibitor tolcapone (SOM0226) in hereditary ATTR amyloidosis patients and asymptomatic carriers: proof-of-concept study#. Amyloid. 2019;26(2):74-84.

40. Sabri O, Seibyl J, Rowe C, Barthel H. Beta-amyloid imaging with florbetaben. Clinical and Translational Imaging. 2015;3(1):13-26.

41. Son HJ, Jeong YJ, Yoon HJ, Lee SY, Choi GE, Park JA, et al. Assessment of brain beta-amyloid deposition in transgenic mouse models of Alzheimer's disease with PET imaging agents 18 F-flutemetamol and 18 F-florbetaben. BMC Neurosci. 2018;19(1).

42. Stenzel J, Rühlmann C, Lindner T, Polei S, Teipel S, Kurth J, et al. [18 F]-florbetaben pet/ct imaging in the alzheimer's disease mouse model APPswe/PS1de9. Current Alzheimer Research. 2019;16(1):49-55.

43. Waldron AM, Verhaeghe J, wyffels L, Schmidt M, Langlois X, Van Der Linden A, et al. Preclinical Comparison of the Amyloid-β Radioligands [11C]Pittsburgh compound B and [18F]florbetaben in Aged APPPS1-21 and BRI1-42 Mouse Models of Cerebral Amyloidosis. Mol Imag Biol. 2015;17(5):688-96.

44. Brendel M, Jaworska A, Grießinger E, Rötzer C, Burgold S, Gildehaus FJ, et al. Cross-sectional comparison of small animal [18F]-florbetaben amyloid-PET between transgenic AD mouse models. PLoS ONE. 2015;10(2).

45. Rominger A, Brendel M, Burgold S, Keppler K, Baumann K, Xiong G, et al. Longitudinal assessment of cerebral β-amyloid deposition in mice overexpressing swedish mutant β-Amyloid precursor protein using 18F-florbetaben PET. J Nucl Med. 2013;54(7):1127-34.

46. Sacher C, Blume T, Beyer L, Peters F, Eckenweber F, Sgobio C, et al. Longitudinal PET monitoring of amyloidosis and microglial activation in a second-generation amyloid-b mouse model. J Nucl Med. 2019;60(12):1787-93.

47. Brendel M, Jaworska A, Herms J, Trambauer J, Rötzer C, Gildehaus FJ, et al. Amyloid-PET predicts inhibition of de novo plaque formation upon chronic γ-secretase modulator treatment. Mol Psychiatry. 2015;20(10):1179-87.

48. Zhang W, Oya S, Kung MP, Hou C, Maier DL, Kung HF. F-18 Polyethyleneglycol stilbenes as PET imaging agents targeting Aβ aggregates in the brain. Nucl Med Biol. 2005;32(8):799-809.

49. Borchelt DR, Ratovitski T, Van Lare J, Lee MK, Gonzales V, Jenkins NA, et al. Accelerated amyloid deposition in the brains of transgenic mice coexpressing mutant presenilin 1 and amyloid precursor proteins. Neuron. 1997;19(4):939-45.

50. Episkopou V, Maeda S, Nishiguchi S, Shimada K, Gaitanaris GA, Gottesman ME, et al. Disruption of the transthyretin gene results in mice with depressed levels of plasma retinol and thyroid hormone. Proc Natl Acad Sci U S A. 1993;90(6):2375-9.

51. Oliveira SM, Ribeiro CA, Cardoso I, Saraiva MJ. Gender-dependent transthyretin modulation of brain amyloid-β Levels: Evidence from a mouse model of alzheimer's disease. J Alzheimer's Dis. 2011;27(2):429-39.

52. Deleye S, Waldron AM, Verhaeghe J, Bottelbergs A, Wyffels L, Van Broeck B, et al. Evaluation of small-animal PET outcome measures to detect disease modification induced by BACE inhibition in a transgenic mouse model of Alzheimer disease. J Nucl Med. 2017;58(12):1977-83.

53. Poisnel G, Dhilly M, Moustié O, Delamare J, Abbas A, Guilloteau D, et al. PET imaging with [18F]AV-45 in an APP/PS1-21 murine model of amyloid plaque deposition. Neurobiol Aging. 2012;33(11):2561-71.

54. Snellman A, Takkinen JS, López-Picón FR, Eskola O, Solin O, Rinne JO, et al. Effect of genotype and age on cerebral [^{18}F]FDG uptake varies between transgenic APP_{Swe}-$PS1_{dE9}$ and Tg2576 mouse models of Alzheimer's disease. Scientific Reports. 2019;9(1).

55. Codita A, Gumucio A, Lannfelt L, Gellerfors P, Winblad B, Mohammed AH, et al. Impaired behavior of female tg-ArcSwe APP mice in the IntelliCage: A longitudinal study. Behav Brain Res. 2010;215(1):83-94.

56. Di Giovanni S, Eleuteri S, Paleologou KE, Yin G, Zweckstetter M, Carrupt PA, et al. Entacapone and tolcapone, two catechol O-methyltransferase inhibitors, block fibril formation of α-synuclein and β-amyloid and protect against amyloid-induced toxicity. J Biol Chem. 2010;285(20):14941-54.

57. Cotrina EY, Gimeno A, Llop J, Jimenez-Barbero J, Quintana J, Valencia G, et al. Calorimetric studies of binary and ternary molecular interactions between transthyretin, Aβ peptides and small-molecule chaperones towards an alternative strategy for Alzheimer's disease drug discovery. J Med Chem. 2020;Submitted.

58. Li X, Masliah E, Reixach N, Buxbaum JN. Neuronal production of transthyretin in human and murine alzheimer's disease: Is it protective? J Neurosci. 2011;31(35):12483-90.

Figures

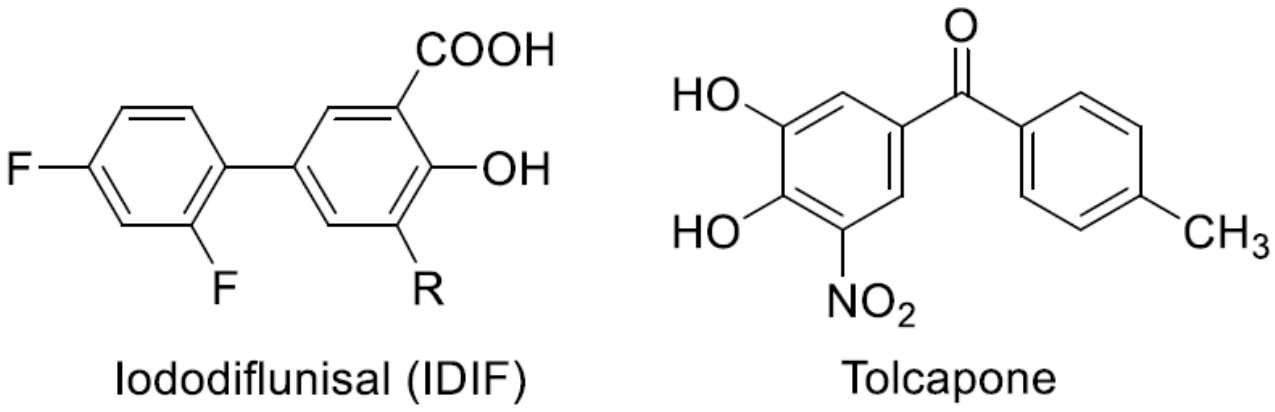

Figure 1

TTR tetramer stabilizers: small T4-like molecules iododiflunisal (IDIF) and repurposed drug tolcapone.

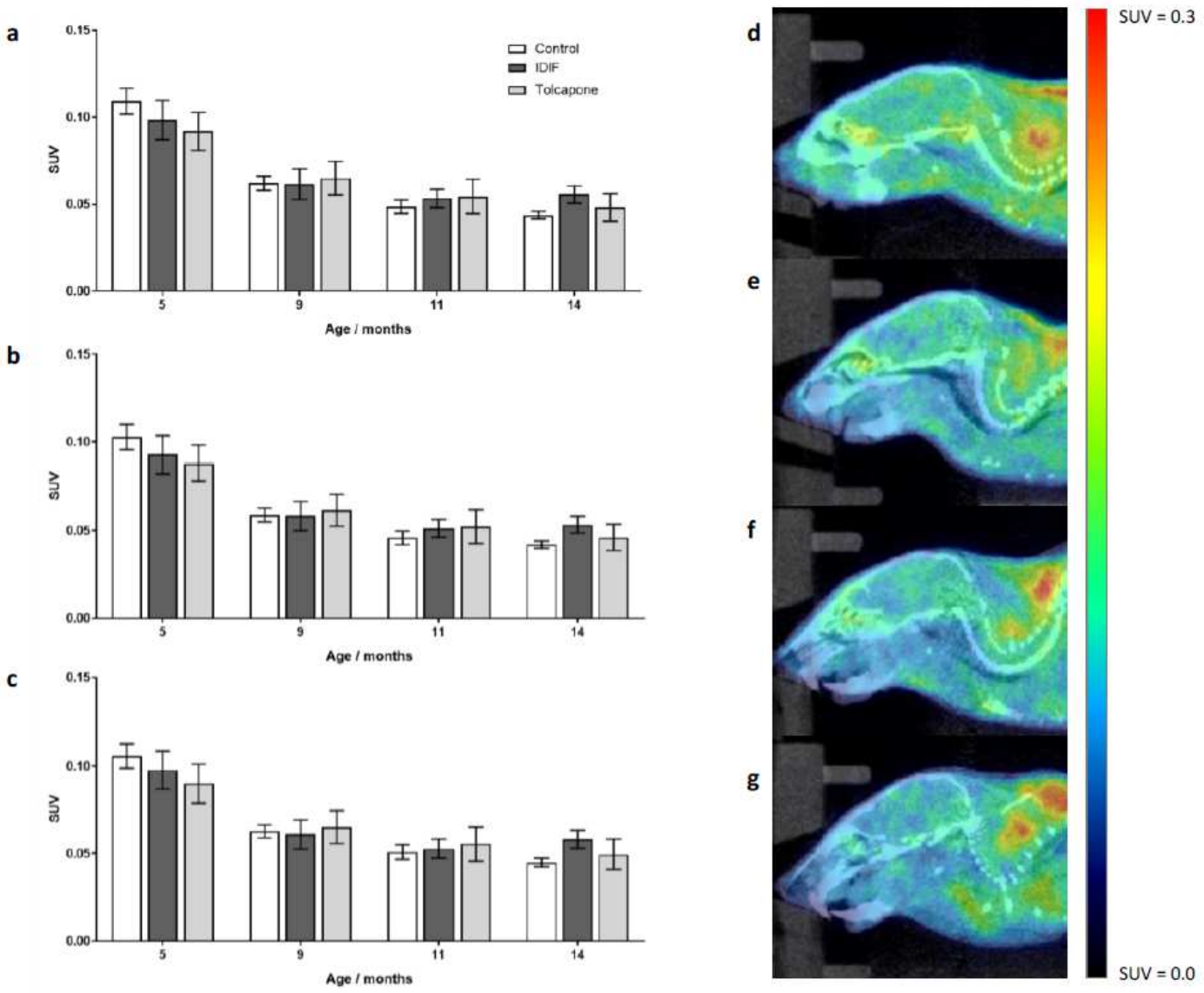

Figure 2

(a–c) SUV values obtained after administration of [18F]florbetaben in: (a) the whole brain; (b) the cortex; and (c) the hippocampus of non-treated, IDIF-treated and tolcapone- treated mice at different ages; (d–g) Representative sagittal PET-CT images obtained at ages of 5 (d), 9 (e), 11 (f) and 14 (g) months after administration of [18F]florbetaben. Images shown correspond to one non-treated animal.

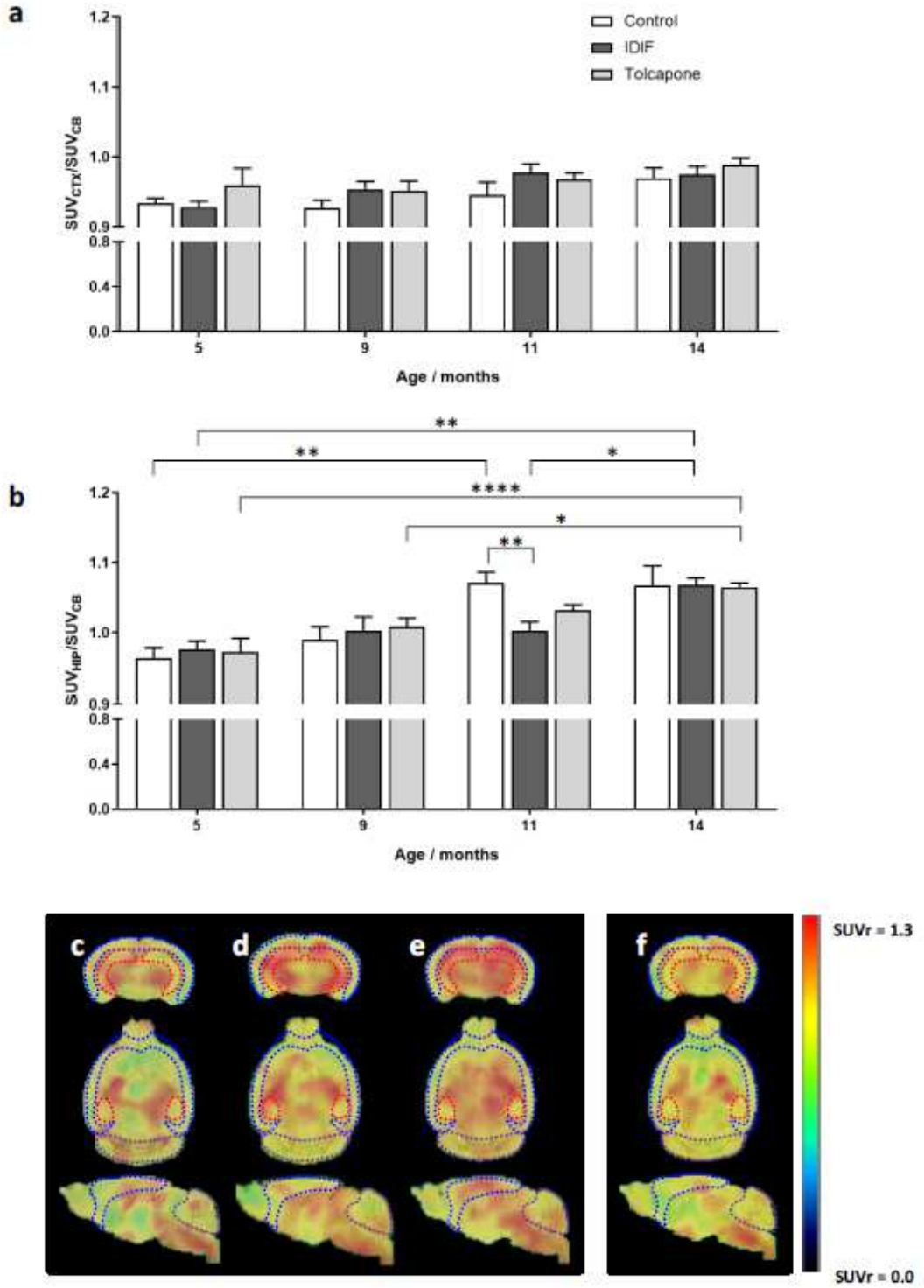

Figure 3

SUVr values (SUV values relative to the cerebellum) in the cortex (a) and the hippocampus (b), obtained after administration of [18F]florbetaben to non-treated, IDIF-treated and tolcapone-treated mice at different ages; (c-f) representative axial, coronal and sagittal PET images corresponding to a non-treated animals at ages=9 (c), 11 (d) and 14 (e) months; (f) representative PET image for an IDIF-treated mouse

at the age of 11 months. PET images have been co-registered with a brain mouse atlas. Volumes of interest drawn in the cortex (blue), hippocampus (red) and cerebellum (brown) are displayed.

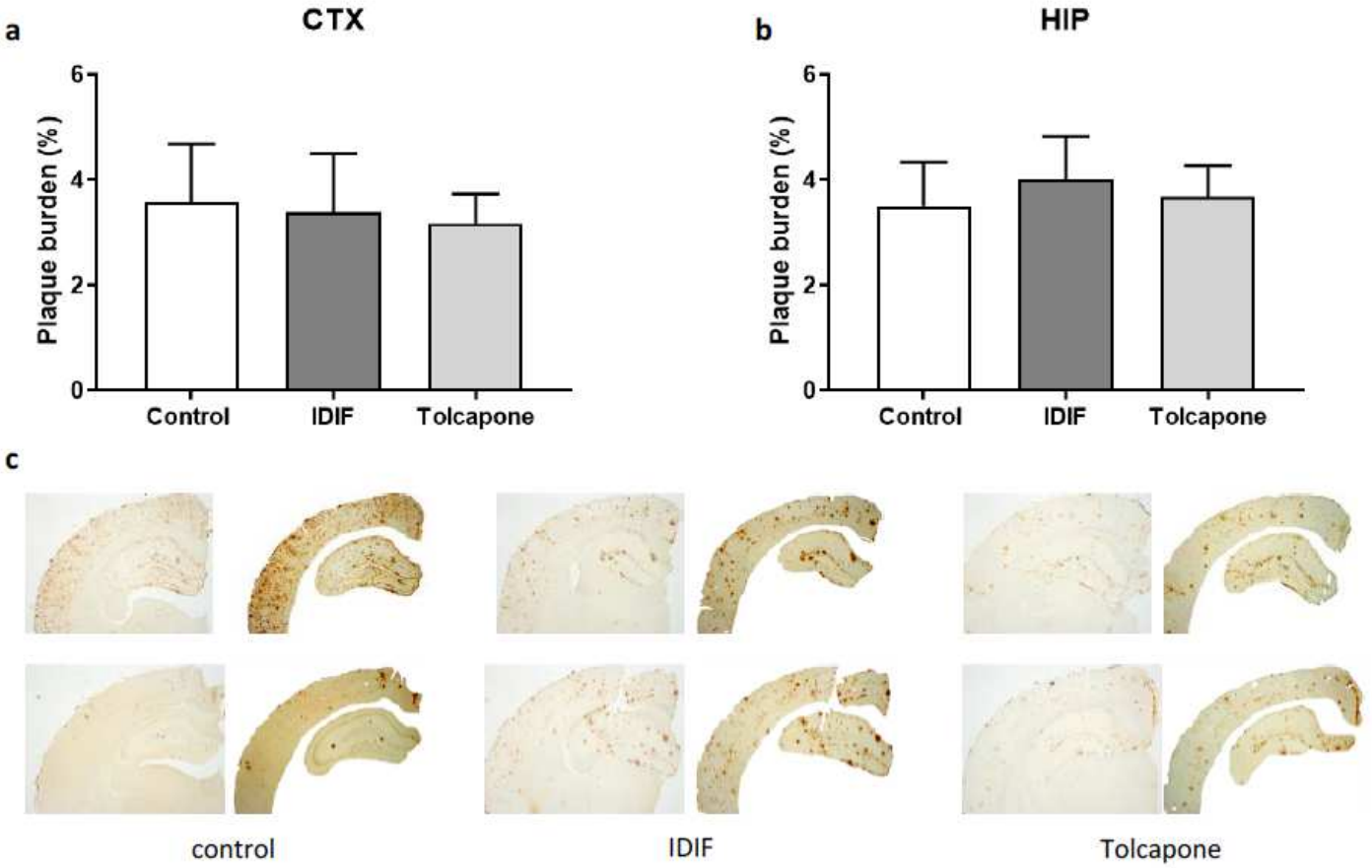

Figure 4

(a, b) Aβ plaque burden in the cortex and hippocampus of non-treated (control), IDIF- treated and tolcapone-treated mice at age=14 months. Error bars represent SEM; (c) photomicrographs illustrate immunohistochemical analysis of brain Aβ plaques using the 6E10 antibody. Brain slices (left) and selected areas for quantification (right) are shown. Slides within each group correspond to two representative animals.